https://onlinelibrary.wiley.com/doi/full/10.1002/cjce.23723
https://doi.org/10.1002/cjce.23723

Cr (VI) adsorption from aqueous solutions on grafted chitosan

Diego O. Sanchez Ramirez[a,*], Monica Periolatto[b], Riccardo A. Carletto[a], Alessio Varesano[a], Claudia Vineis[a], Cinzia Tonetti[a], Roberta Bongiovanni[b]

[a] *Istituto di Sistemi e Tecnologie Industriali Intelligenti per il Manufatturiero Avanzato (STIIMA), National Research Council of Italy, Biella, 13900, Italy*
[b] *Politecnico di Torino – Dipartimento di Scienza Applicata e Tecnologia, Turin, 10129, Italy*
**Corresponding author E-mail: diegoomar.sanchezramirez@stiima.cnr.it*

ABSTRACT

Chitosan was grafted on the surface of a cotton gauze (20, 50 and 100 mg chitosan g^{-1} cotton) to improve its stability in aqueous solutions. The adsorption of hexavalent chromium ions from water on the grafted chitosan was evaluated to determine, by means of linear and nonlinear models, the kinetic and isotherm adsorption of the process. Kinetics of pseudo second-order, pseudo first-order and adsorption isotherm type II were obtained, that is, a monolayer adsorption on nonporous adsorbents with physical adsorption was present. The most probable energy of adsorption corresponded to a physisorption with hydrogen bond interactions between chromium ions and ammonium groups. Moreover, three different cross-sectional areas of hexavalent chromium ions were calculated and used to estimate the specific surface area employed by active sites to adsorb metal ions in terms of chitosan or cotton mass. Finally, a percentage of area occupied by chromium ions on surface was approached dividing the resulting specific surface area in terms of cotton mass by the specific surface area of cotton reported in literature. As a result, it was approached that the occupied area is between 6 % (for 20 mg chitosan g^{-1} cotton) and 24% (for 100 mg chitosan g^{-1} cotton) from the total area of cotton.

KEYWORDS chromium removal, adsorption, chitosan, specific surface area, cross-sectional area.

INTRODUCTION

Hexavalent chromium (Cr (VI)), is a toxic form of the valence states of the element chromium. It is produced either by the natural oxidation of chromium III or by anthropogenic activities [1-3]. The latter one is the main cause of Cr (VI) pollution, when is added to alloy steel or when is used as anticorrosive agent or pigments in dyes, paints, inks and plastics [1]. It is said that Cr (VI) can cause liver damage, reproductive problems, cancer in the respiratory system (classification in the International Agency for Research on Cancer - Group 1[4]) and affect kidneys, skin and eyes [1, 5]. According to the World Health Organization (WHO), the guideline concentration of Cr (VI) in

drinking water should reach a maximum of 50 μg l^{-1}, which is however a provisional value established by WHO due to uncertainties in toxicological data [6, 7]. In addition, the literature reports that the consumption of Cr (VI) in drinking water, at the concentration of 180 mg l^{-1}, can provoke cancer in the small intestine of mice [3]. Likewise, it is worth highlighting that Cr (VI) pollution in drinking water is a problem caused mainly by the contamination of wells and ground water [2, 3, 8]. In order to remove heavy metal from aqueous solutions, conventional methods can be used: chemical precipitation and filtration, electrochemical treatments, ion exchange and reverse osmosis. Nevertheless, these methods are costly and adsorption is proposed as an alternative to remove heavy metals from wastewaters by using adsorbent materials of mineral, organic or biological origin [9]. Low cost adsorbents of natural origin are noteworthy. The attention can be also focused on substrates derived from various natural sources such as agricultural waste, industrial by-products, natural materials or modified biopolymers [10].

Among the adsorbents of natural origin, in recent years chitosan is gaining great interest thanks to its multiple applications [11]. Chitosan is a polysaccharide of β (1-4) linked D-glucosamine and N-acetyl-D-glucosamine and it is the second most abundant natural biopolymer after cellulose. The interest in chitosan as adsorbent is due to the presence of amino groups, which can act as sites to bond heavy metal ions [12, 13]. In addition, in order to improve the chitosan stability in aqueous solutions, this biopolymer can be crosslinked or grafted onto solid substrates [14]. The efficiency of chitosan to remove metal ions is retained when it is UV-grafted onto the cotton surface [15]. The experiment has suggested that the free amino groups of chitosan are not involved in the radical grafting of chitosan but remained available to bond metal ions [15–17].

The aim of this study is to determine which kinetic model (Lagergren's pseudo-first-order or Ho's pseudo-second-order) and which isotherm adsorption (Langmuir, Freundlich, Dubinin-Radushkevich and BET) is more adequate to describe the adsorption of Cr (VI) ions on grafted chitosan. To determine the parameters of kinetic and isotherm adsorption, the linear and nonlinear equations of models were employed. In addition, the specific surface area occupied by metal ions was estimated using the adsorption capacity of BET model. The presence of Cr (VI) on the adsorbent material was studied with Energy Dispersive X-ray Spectroscopy (EDS). In order to study any chemical modification on the adsorbent material after adsorption tests FT-IR analyses were carried out. Finally, the viscosity average molecular weight of chitosan was determined.

MATERIALS AND METHODS

Chitosan low molecular weight (C_{LMW}) with 75 – 85 % deacetylation degree was purchased from Sigma Aldrich S.r.l. (Milano, Italy). Irgacure 1173 (BASF Corporation, Florham Park, NJ, USA) was used as radical photoinitiator and pure cotton gauze (COT) (49 g m^{-2} with hexagonal holes of 2 mm opening) was employed as substrate.

The viscosity average molecular weight of chitosan was estimated by measuring the reduced viscosity of standard solutions at four different concentrations (0.01, 0.04, 0.07 and 0.10 g dl^{-1}). These chitosan solutions were prepared in accordance with the method reported in literature [18]. The measure of viscosity was carried out with a cone-on-plate Anton Paar Physica MCR 301 rotational rheometer (Austria). The surface of the cone plate system was heated to the temperature of 25 °C by a heat-exchanger Heater Unit H-PTD 200 (Anton Paar Austria). The spindle of the cone plate system was equipped with a cone model CP 75-1 with a diameter of 75 mm and an angle of 1°. The value of the intrinsic viscosity at the intersection of the fitting straight line was calculated. Then, the Mark-Houwink equation was employed and the constants values were selected according to the solvent system applied; *K* and *a* are equal to 15.7×10^{-3} cm^3 g^{-1} and 0.79, respectively [18].

For the adsorption tests a stock Cr (VI) solution of 1000 mg l^{-1} was prepared by dissolving a proper amount of $K_2Cr_2O_7$ (Sigma Aldrich) in distilled water. Metal solutions at lower concentrations used in the experiments, namely 10, 50, 100, 150 and 250 mg l^{-1}, were prepared by dilution of the stock.

Sample Preparation

Cotton gauzes (COT) were functionalized by C_{LMW} according to the procedure previously reported in literature [19]. The main parameters are hereafter summarized: the gauze was dipped in a proper amount of chitosan solution and photoinitiator, enough to reach the desired add-on: 20, 50 and 100 mg C_{LMW} g^{-1} COT. After a contact time of 12 h, it was dried and UV irradiated on both sides for 60 s in inert atmosphere, providing an irradiance of about 60 mW cm^{-2} followed by a conditioning step at 20 °C and 65 %RH for 24 h. Additional information about the characterizations (SEM, FT-IR, TGA and AFM analyses) of the absorbents can be found in literature [19, 20].

Adsorption Tests

The adsorption tests were carried out on the prepared samples, at pH 3 and 20 °C. These parameters were fixed considering the best performing parameters of a previous study [19]. The adsorbent material (COT-C_{LMW}) was sealed in test tubes and stirred with the metal solution at the ratio of 100 mg of COT-C_{LMW}: 10 ml of liquid, varying the contact time and the initial concentration of Cr (VI). The concentration of Cr (VI) in the supernatant was determined by 1,5-diphenylcarbazide method - United States Environmental Protection Agency (EPA), Method 7196A: Chromium, Hexavalent (Colorimetric), part of Test Methods for Evaluating Solid Waste, Physical/Chemical Methods, July 1992 - using a UV-Visible Spectrometer (Lambda 35 PerkinElmer). The adsorption tests were repeated three times and results were averaged.

The adsorption capacity of the adsorbent q_t (mg Cr (VI) g^{-1} COT-C_{LMW}), at a given time t, is defined as the amount of adsorbed metal per mass unit of adsorbent material (COT-C_{LMW}). It was evaluated according the Equation (1):

$$q_t = \frac{(C_0 - C_t) \cdot V}{m} \quad (1)$$

where C_0 and C_t (mg Cr (VI) l^{-1}) are the metal concentrations in solution at time zero and at time t respectively, V (l) is the volume of the metal solutions (10 ml) and m (g) is the mass of adsorbent material (100 mg COT-C_{LMW}). The presence of Cr (VI) on the adsorbent material was verified by using EDS with an Oxford Instrument Model 7060 Link ISIS. In addition, IR spectra before and after adsorption tests were recorded to study any chemical modification caused by the adsorption of Cr (VI). In FT-IR analyses, a Thermo Nicolet iN10 spectrometer equipped with iZ10 module by an attenuated total reflection technique with a Smart Endurance accessory (equipped with a diamond crystal ZnSe focusing element) was used in the range from 4000 to 650 cm^{-1} with 100 scans and 4 cm^{-1} band resolution.

Adsorption Kinetics

The adsorption experimental data were fitted to the Lagergren's pseudo-first-order [21–23] and Ho's pseudo-second-order models [24–26]. The linear and nonlinear pseudo-first-order equation is represented by Equation (2.1) and (2.2), while the linear and nonlinear pseudo-second-order is expressed in Equation (3.1) and (3.2):

$$\log(q_e - q_t) = \log(q_e) - \frac{K_1 \cdot t}{2.303} \quad (2.1)$$

$$q_t = q_e \cdot (1 - e^{K_1 \cdot t}) \quad (2.2)$$

$$\frac{t}{q_t} = \frac{1}{K_2 \cdot {q_e}^2} + \frac{t}{q_e} \quad (3.1)$$

$$q_t = \frac{K_2 \cdot {q_t}^2 \cdot t}{1 + q_e \cdot K_2 \cdot t} \quad (3.1)$$

where q_e (mg Cr (VI) g^{-1} COT-C_{LMW}) is the amount of metal ion adsorbed at the equilibrium time, K_1 (min^{-1}) and K_2 (g mg^{-1} min^{-1}) are the rate constant of the equations, respectively.

Adsorption Isotherms

Langmuir isotherm model [27] is based on the assumption of monolayer adsorption on chemisorption or physisorption process. The linear and nonlinear equation are written in Equations (4.1) and (4.2). Despite the fact that four linearized forms of the Langmuir's model were used (Hanes-Woolf, Lineweaver-Burke, Eadie-Hofstee, and Scatchard), the Hanes-Woolf's linearization (Equation 4.1) was the best match for the parameters of non-linear equation. For the complete results of those linearized forms see the Supporting File.

$$\frac{C_e}{q_e} = \frac{1}{q_m \cdot K_L} + \frac{C_e}{q_m} \quad (4.1)$$

$$q_e = \frac{q_m \cdot K_L \cdot C_e}{1 + K_L \cdot C_e} \quad (4.2)$$

where q_m (mg Cr (VI) g^{-1} COT-C_{LMW}) is the maximum adsorption capacity of the adsorbent on the formed monolayer and K_L (l mg^{-1}) is the Langmuir adsorption constant.

Freundlich isotherm model [28, 29] is an empirical equation applied on chemisorption and physisorption process at low coverages. It requires low values of C_e, otherwise, q_e tends to the asymptotic maximum of saturation. The linear and nonlinear equation are written in Equation (5.1) and (5.2):

$$\log(q_e) = \log(K_f) + \frac{\log(C_e)}{n} \quad (5.1)$$

$$q_e = K_f \cdot {C_e}^{1/n} \quad (5.2)$$

where n is an empirical and dimensionless parameter relating to the adsorption intensity and K_f (mg g^{-1} $l^{1/n}$ $mg^{-1/n}$) is a constant relating to the adsorption capacity.

Dubining-Raduschkevich (D-R) isotherm model [30–33] can be applied to express the adsorption mechanism, chemical or physical, with monolayer formation and Gaussian energy distribution onto a surface. The linear and nonlinear form of this model are represented by Equation (6.1) and (6.2):

$$\ln(q_e) = \ln(q_m) - B \cdot \varepsilon^2 \quad (6.1)$$

$$q_e = q_m \cdot e^{-B \cdot \varepsilon^2} \quad (6.2)$$

where B is a constant related to the energy of adsorption ($mol^2\ kJ^{-2}$) and ε is the Polanyi potential of adsorption process. The Polanyi potential (ε) can be calculated from Equation (6.3) [34–37]:

$$\varepsilon = R \cdot T \cdot \ln\left(\frac{C_{sat}}{C_e}\right) \quad (6.3)$$

where R is the universal gas constant ($kJ\ mol^{-1}\ K^{-1}$), T is the temperature (293.15 K) and C_{sat} is the concentration of saturation.

The term B can be used to estimate the most probable energy of adsorption (E, in $kJ\ mol^{-1}$) [38] by Equation (6.4):

$$E = (2 \cdot B)^{-1/2} \quad (6.4)$$

BET isotherm model [39, 40] is an extension of the Langmuir model and it is applied on physisorption process with multilayer formation. In this case, BET model was used to determine q_m which was successively employed to estimate the specific surface area as reported in literature [41, 42]. The linear and nonlinear forms of this equation are presented in Equations (7.1) and (7.2), respectively. It is expressed in terms of concentration applying the ideal gas equation.

$$\frac{C_e/C_{sat}}{q_e \cdot \left(1 - C_e/C_{sat}\right)} = \frac{1}{c * q_m} + \frac{(c-1) \cdot \left(C_e/C_{sat}\right)}{c \cdot q_m} \quad (7.1)$$

$$q_e = \frac{c \cdot q_m \cdot \left(C_e/C_{sat}\right)}{\left(1 - C_e/C_{sat}\right) \cdot \left(1 - C_e/C_{sat} + c \cdot \left(C_e/C_{sat}\right)\right)} \quad (7.2)$$

where c is a term associated to the adsorption enthalpy of first and subsequent layers.

Linear and Nonlinear Regressions

Kinetic and isotherm parameters were determined by linear and nonlinear regressions using Microsoft Excel®. The best fitting linear regressions were estimated with the highest coefficient of determination (R^2). To obtain the best fitting nonlinear regressions, the minimization of residual sum of squares (RSS) was realized using the add-in program Solver in Microsoft Excel®. Finally, the Akaike's Information Criterion (AIC) was employed to compare nonlinear models. AIC for model comparisons can be represented by the Equation (8)

$$AIC = 2 \cdot k + N \cdot \log\left(\frac{RSS}{N}\right) \quad (8)$$

where N is the number of observations and k is the number of parameters.

Cross-Sectional Area and Specific Surface Area

The specific surface area per mass was estimated with the Equation (9) [42]:

$$A_s = \frac{q_{mBET} \cdot N_A \cdot \sigma}{M} \quad (9)$$

where A_s is the specific surface area, N_A is the Avogadro number (6.02×10^{23} molecule mol^{-1}), σ is the cross-sectional area of a single molecule (in the plane of adsorbent surface) and M is the molecular weight. The adsorption capacity ($q_{m,BET}$) was expressed in mg Cr (VI) g^{-1} C_{LMW} instead of mg Cr (VI) g^{-1} COT-C_{LMW} to consider the real action of chitosan. The cross-sectional area of a single molecule of Cr (VI) was calculated in three different ways.

The first one, the solid density of chromic acid (H_2CrO_4, CAS No. 7738-94-5) was employed according to the following Equation (9.1) [43, 44]:

$$\sigma_1 = 1.091 \cdot \left(\frac{M}{\rho \cdot N_A}\right)^{2/3} \quad (9.1)$$

where M is the molecular weight (118.01 g mol^{-1}), ρ is the density (2.29 g cm^{-3}) [45] and 1.091 is the hexagonal packing factor and σ_1 (m^2 $molecule^{-1}$) is the cross-sectional area calculated by density.

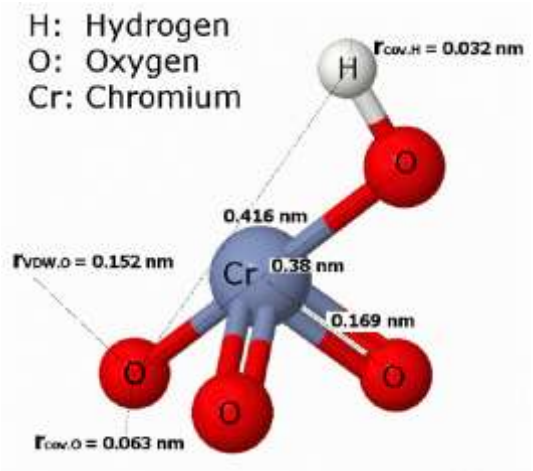

Figure 1. Molecular structure of $HCrO_4^-$ and distances between atoms, Jensen et al.[46]; $r_{COV.H}$: Covalent radius-Hydrogen, $r_{COV.O}$: Covalent radius-Oxygen and $r_{VDW.O}$: Van der Waals radius-Oxygen

The second one, the greatest distance (Figure 1) between atoms (0.416 nm) in the chromic acid molecule plus their corresponding covalent radius (0.032 nm and 0.063 nm for hydrogen and oxygen, respectively) [46, 47] were used as diameter; the Equation (9.2) of the area of a circle was used as the cross-sectional area:

$$\sigma_2 = \left(\frac{\pi}{4}\right) \cdot {d_1}^2 \quad (9.2)$$

where d_1 is the diameter (0.511 nm) and σ_2 (m^2 $molecule^{-1}$) is the cross-sectional area calculated by considering covalent radius only.

Lastly, the greatest distance (Figure 1) between atoms (0.416 nm) in the chromic acid molecule [46] plus the covalent radius of hydrogen (0.032 nm) [47] more the Van der Waals radius of oxygen (0.152 nm) [48] were used as diameter; the Equation (9.3) of the area of a circle was used as the cross-sectional area in this case as well:

$$\sigma_3 = \left(\frac{\pi}{4}\right) \cdot {d_2}^2 \qquad (9.3)$$

where d_2 is the diameter (0.600 nm) and σ_3 (m^2 $molecule^{-1}$) is the cross-sectional area calculated by considering one covalent radius (hydrogen) and one Van der Waals radius (oxygen).

RESULTS AND DISCUSSION

The average molecular weight of chitosan employed in this work was measured. For this purpose, the measurement of standard solution viscosity at four different concentrations, according to the procedure described in the section of Materials and Methods, reported that the intrinsic viscosity was equal to 4.40 dl g^{-1} and the corresponding viscosity average molecular weight calculated from the Mark-Houwink equation was 4.26×10^5 Da with R^2 of 0.9992.

The adsorption of Cr (VI) was evaluated first on COT without C_{LMW}, in the same conditions as the samples treated with chitosan: pristine COT was immersed in solutions of Cr (VI) at different concentrations (10, 50, 100, 150 and 200 mg Cr (VI) l^{-1}) and the metal concentration was monitored after 24 h. The results showed, as expected, that pristine cotton had not adsorbed chromium ions from aqueous solutions. The adsorption experiments were repeated with the modified COT by C_{LMW} UV-grafting. Figure 2 reports the spectrum EDS and the spectra FT-IR.

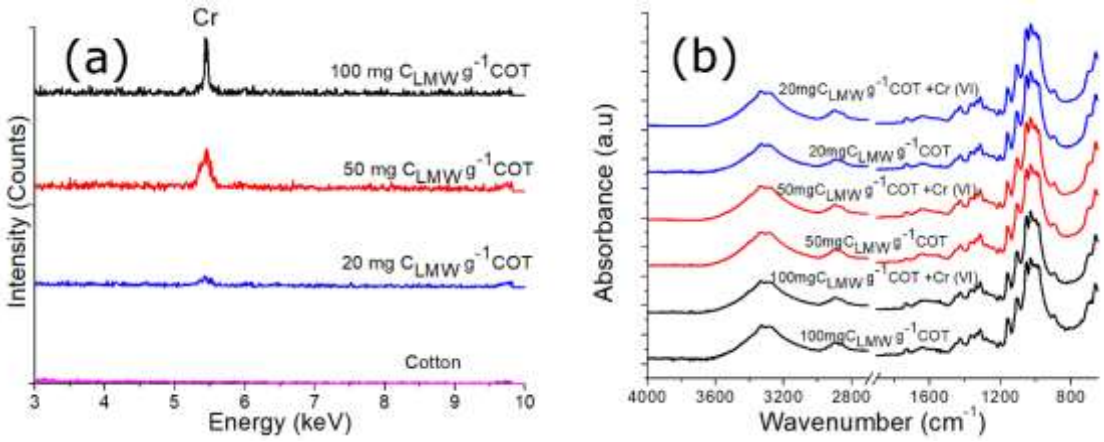

Figure 2. Spectra (a) EDS and (b) FT-IR after 24 h at the initial concentration of 200 mg Cr (VI) l^{-1}

On one hand, Figure 2(a) qualitatively confirms the presence of Cr (VI) ions on the cotton gauze grafted with C_{LMW} after immersion in solution, while COT did not demonstrate the adsorption of Cr (VI). In addition, a reduction on intensity of chromium was evidenced when the amount of chitosan on cotton gauze was reduced. On the other hand, Figure 2(b) shows that the presence of Cr (VI) on the adsorbent material does not produce or modify any peak in the spectra. The typical peak of chitosan at 1560 cm^{-1} [19] caused by the bending of NH amide group was not satisfactorily evidenced by this instrumental analysis. It is a consequence of small concentrations of chitosan on cotton surface.

In Figure 3(a), the adsorption capacity (q_t) of adsorbent material at different add-on of C_{LMW} (20, 50 and 100 mg C_{LMW} g^{-1} COT) is reported as a function of time (with 100 mg Cr (VI) l^{-1} as the initial concentration). As it shows, the equilibrium conditions were reached after approximatively one hour.

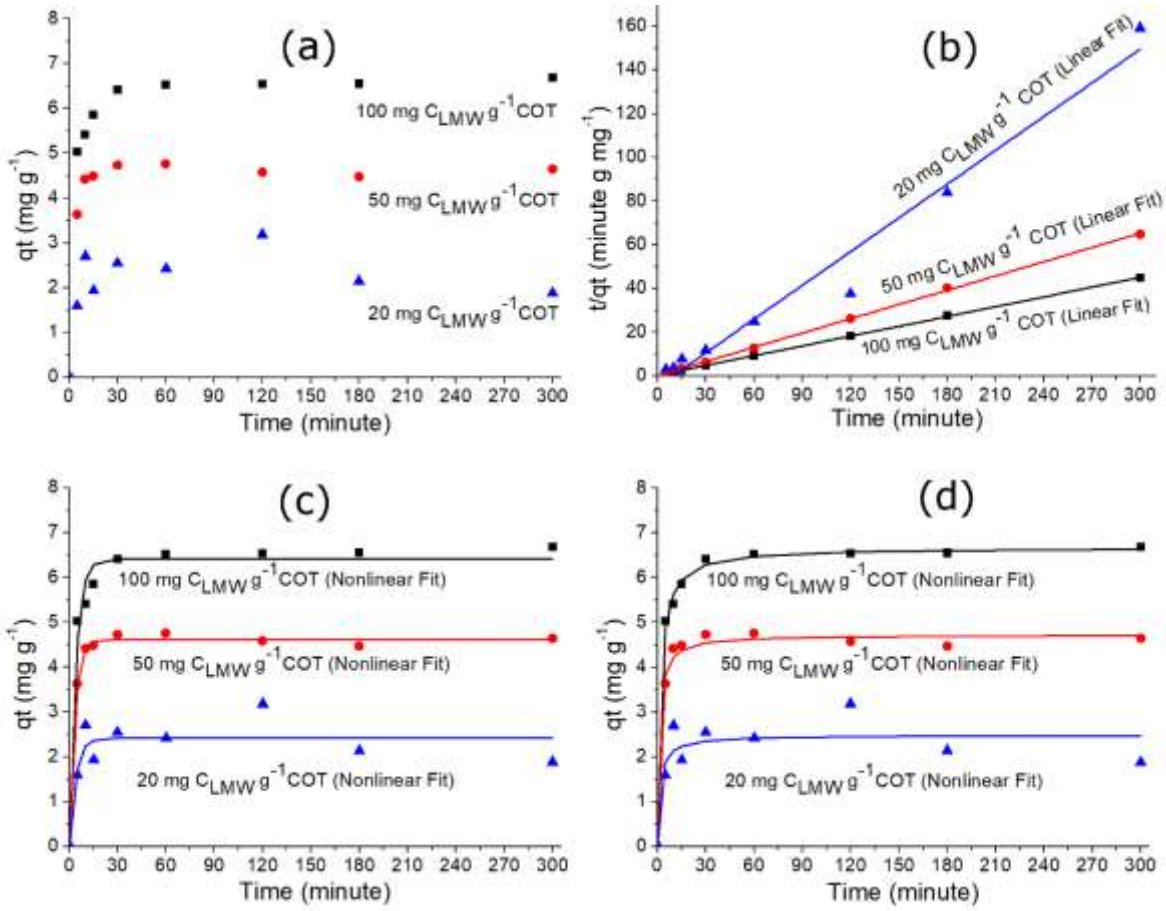

Figure 3. (a) Adsorption capacity as a function of time at the initial concentration of 100 mg Cr (VI) l^{-1}. Fitting of experimental data by: (b) pseudo-second order from linear model, (c) pseudo-first order from nonlinear model, (d) pseudo-second order from nonlinear model.

Resulting R^2, RSS and *AIC* (Table 1) indicate that the adsorption kinetics of Cr (VI) on the adsorbents are represented by the models of pseudo-second (Figure 3(b) and (3(d)) and pseudo-first order (Figure 3(c)) for 100 and 50 – 20 mg C_{LMW} g^{-1} COT, respectively. The cause of these results is probably the reduction of chitosan concentration on the surface of cotton gauze. Small concentration of chitosan on the surface of cotton (50 – 20 mg C_{LMW} g^{-1} COT) induces the presence of a model of pseudo-first order and higher concentration of chitosan (100 mg C_{LMW} g^{-1} COT) gives rise to a kinetic of pseudo-second order. The last result is in agreement with previous results where the add-on of chitosan was between 100 and 300 mg C_{LMW} g^{-1} COT [19].

Table 1. Kinetic parameters of linear and nonlinear models according to pseudo-first and pseudo-second order

Model	Parameter	100 mg C_{LMW} g^{-1} COT	50 mg C_{LMW} g^{-1} COT	20 mg C_{LMW} g^{-1} COT
Lagergren Linear	K_1 (min^{-1})	0.0020	0.0005	0.0003
	q_{e1} (mg g^{-1})	2.2440	2.0692	0.8722
	R^2	0.5204	0.1059	0.0014
Lagergren Nonlinear	K_1 (min^{-1})	0.2569	0.3059	0.2589
	q_{e1} (mg g^{-1})	6.4204	4.6201	2.4162
	RSS	0.7051	0.0648	1.3968
	AIC	-2.4385	-10.7311	-0.0637
Ho Linear	K_2 (g mg^{-1} min^{-1})	0.0704	0.5093	0.0551
	q_{e2} (mg g^{-1})	6.7007	4.6030	1.9440
	R^2	0.9999	0.9995	0.9738
Ho Nonlinear	K_2 (g mg^{-1} min^{-1})	0.0817	0.1800	0.2517
	q_{e2} (mg g^{-1})	6.6690	4.7257	2.4834
	RSS	0.1024	0.2019	1.5140
	AIC	-9.1437	-6.7840	0.2163

As regards the add-on of 100 g C_{LMW} g^{-1} COT with a kinetic model of pseudo-second order, good fitting was obtained in both linear and nonlinear models; similar results of q_{e2} and K_2 were achieved in both cases. On the other hand, the add-on of 50 and 20 mg C_{LMW} g^{-1} COT with models of pseudo-first order showed different results for linear and nonlinear models with the worst fitting in the linear case. As a result, it can be said that the loss of information produced by the linearization of kinetic equations is considerable only when the add-on of chitosan is between 50 and 20 mg C_{LMW} g^{-1} COT.

Table 2. Mechanism and kinetic rate of adsorption of Cr (VI) on grafted chitosan

Mechanism	
$P\text{-}NH_2H^+_{(s)} + HCrO_4^-{}_{(aq)} \leftrightarrow P\text{-}NH_2H^{+\cdots}HCrO_4^-{}_{(s)}$	
Kinetic rates	
Order	Add-on
$dq_t/dt = K_1 (q_e - q_t)$	$\leq$ 50 mg C_{LMW} g^{-1} COT
$dq_t/dt = K_2 (q_e - q_t)^2$	$\geq$ 100 mg C_{LMW} g^{-1} COT*

*Considering results previously reported in literature, Ferrero et al.[19].

In addition, it is known that the most stable and dominant form of Cr (VI) at pH 3.0 and concentration < 200 mg Cr (VI) l^{-1} is $HCrO_4^-{}_{(aq)}$ [49, 50]. Also, it is necessary to remember that in an acidic ambient, the surface charges of chitosan vary with an increase of the positive charge of the adsorbent due to the protonation of amine groups to form ammonium groups, that is to say $P\text{-}NH_{2\,(sol)}$ to $P\text{-}NH_2H^+_{(s)}$, where $P\text{-}NH_2H^+_{(s)}$ is the polar site on the surface of C_{LMW}. Consequently,

the overall mechanism and kinetics of adsorption for Cr (VI) ions on grafted chitosan could be summarized as reported in Table 2.

The adsorption isotherm model of metal ions in solution was investigated using as initial concentration 10, 50, 100, 150 and 200 mg Cr (VI) l^{-1}. The values of the concentration (C_e) and the adsorption capacity (q_e) of Cr (VI), at 24 h contact time between adsorbent material and metal ions, are reported in Figure 4. This figure demonstrates that Type II adsorption isotherms (IUPAC Classification [41, 51]) were obtained. The initial steep rise of q_e confirmed the complete formation of monolayer coverage. Consequently, these isotherms are the result of unrestricted monolayer adsorption on nonporous or macroporous adsorbents during a physisorption process [41, 51].

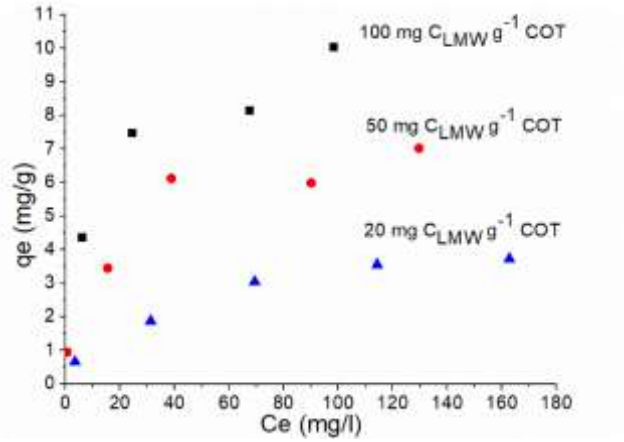

Figure 4. Experimental adsorption isotherms of Cr (VI) on grafted chitosan, at 24 h of contact time between chromium solution and adsorbent material in batch condition

The experimental data were fitted with the isotherm models of Langmuir, Freundlich, D-R and BET. The curves of linear (Equation 4.1, 5.1, 6.1 and 7.1) and nonlinear (Equation 4.2, 5.2, 6.2 and 7.2) regressions are reported in Figure 5 and Figure 6, respectively. All resulting parameters are indicated in Table 3. According to the values of R^2, RSS and *AIC* (Table 3), the model of Langmuir in all add-on cases can better describe the adsorption of Cr (VI) ions. Nevertheless, the models of Freundlich and D-R reported a good fitting, mainly when the add-on of chitosan was reduced to 20 mg C_{LMW} g^{-1} COT.

Table 3. The adsorption parameters of linear and nonlinear isotherm models

Model	Parameter	100 mg C_{LMW} g^{-1} COT	50 mg C_{LMW} g^{-1} COT	20 mg C_{LMW} g^{-1} COT
Langmuir*	q_m (mg g^{-1})	10.2620	7.2431	4.3754

Linear	K_L (l mg^{-1})	0.1165	0.0979	0.0345
	R^2	0.9818	0.9816	0.9836
Langmuir Nonlinear	q_m (mg g^{-1})	10.0068	7.6051	4.7343
	K_L (l mg^{-1})	0.1245	0.0661	0.0245
	RSS	1.3479	1.3949	0.1357
	AIC	3.1535	3.2279	-1.8316
Freundlich Linear	K_f (mg g^{-1} l$^{1/n}$ mg$^{-1/n}$)	1.4633	1.2555	0.3846
	n	2.2385	2.7046	2.1532
	R^2	0.9440	0.9740	0.9902
Freundlich Nonlinear	K_f (mg g^{-1} l$^{1/n}$ mg$^{-1/n}$)	2.3151	1.6520	0.4823
	n	3.1398	3.3177	2.4206
	RSS	2.7249	1.7876	0.1778
	AIC	4.6819	3.7665	-1.2448
D-R Linear	q_m (mg g^{-1})	8.5648	5.8744	3.2946
	B (mol^2 kJ^{-2})	0.0166	0.0118	0.0185
	R^2	0.9894	0.9477	0.9541
	E (kJ mol^{-1})	5.4907	6.5111	5.2001
D-R Nonlinear	q_m (mg g^{-1})	9.1018	6.6546	3.6138
	B (mol^2 kJ^{-2})	0.0158	0.0202	0.0343
	RSS	1.6319	1.5278	0.3023
	AIC	3.5686	3.4254	-0.0929
	E (kJ mol^{-1})	5.6262	4.9770	3.8176
BET Linear**	q_m (mg g^{-1})	6.1664	4.4462	1.8376
	c	30.3168	31.0977	23.5663
	R^2	0.9999	0.9717	0.9992
BET Nonlinear**	q_m (mg g^{-1})	6.1667	4.9904	1.8270
	c	30.2989	12.9128	24.5822
	RSS	0.0000	0.5295	0.0044
	AIC	-13.0798	3.7403	-0.0929

*These results were obtained by using the Hanes-Woolf's linearization of Langmuir equation. For more information see Supporting File.

** In this model only $C_e/C_{sat} < 0.45$ was considered

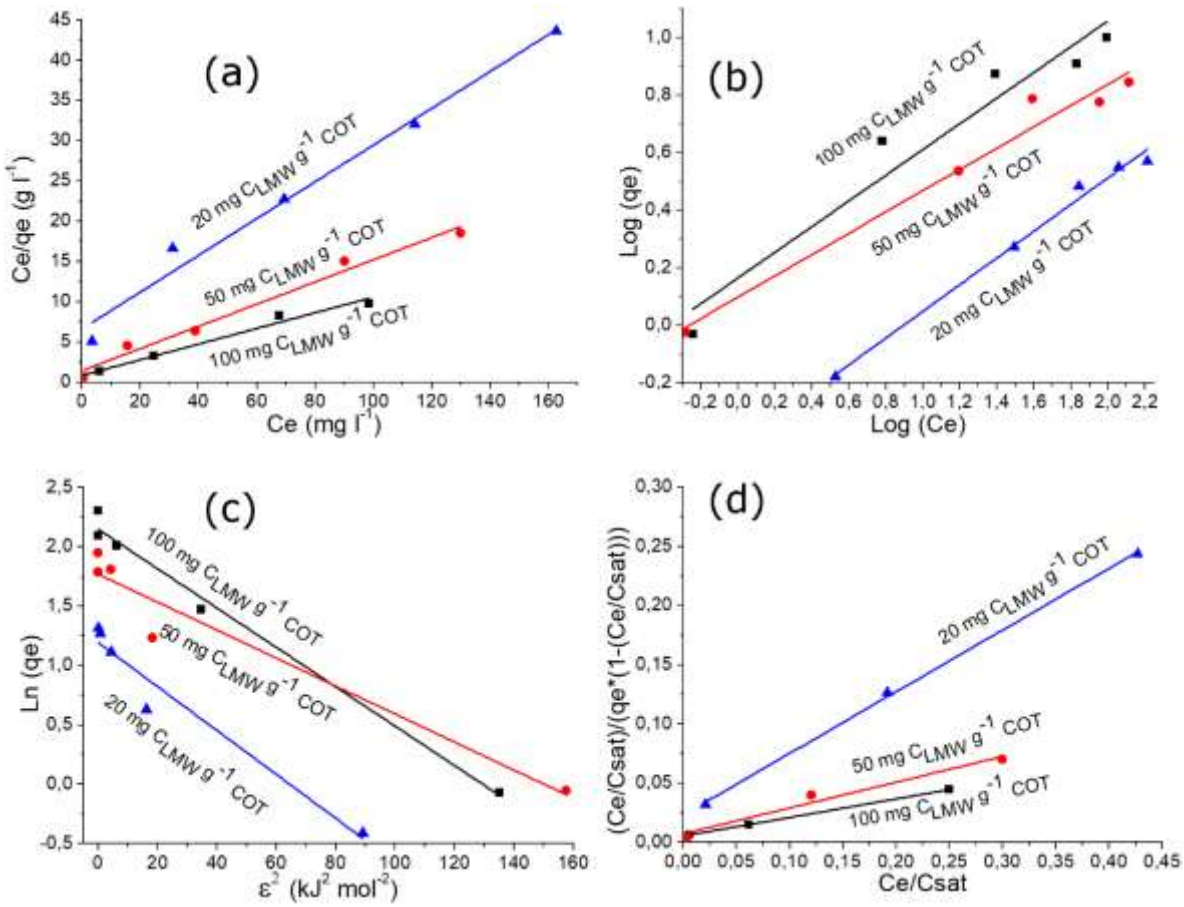

Figure 5. Linear regressions of isotherm models: (a) Langmuir - Equation 4.1, (b) Freundlich - Equation 5.1, (c) D-R - Equation 6.1 and (d) BET - Equation 7.1. The main parameters of each linear model and the values of R^2 are reported in Table 3.

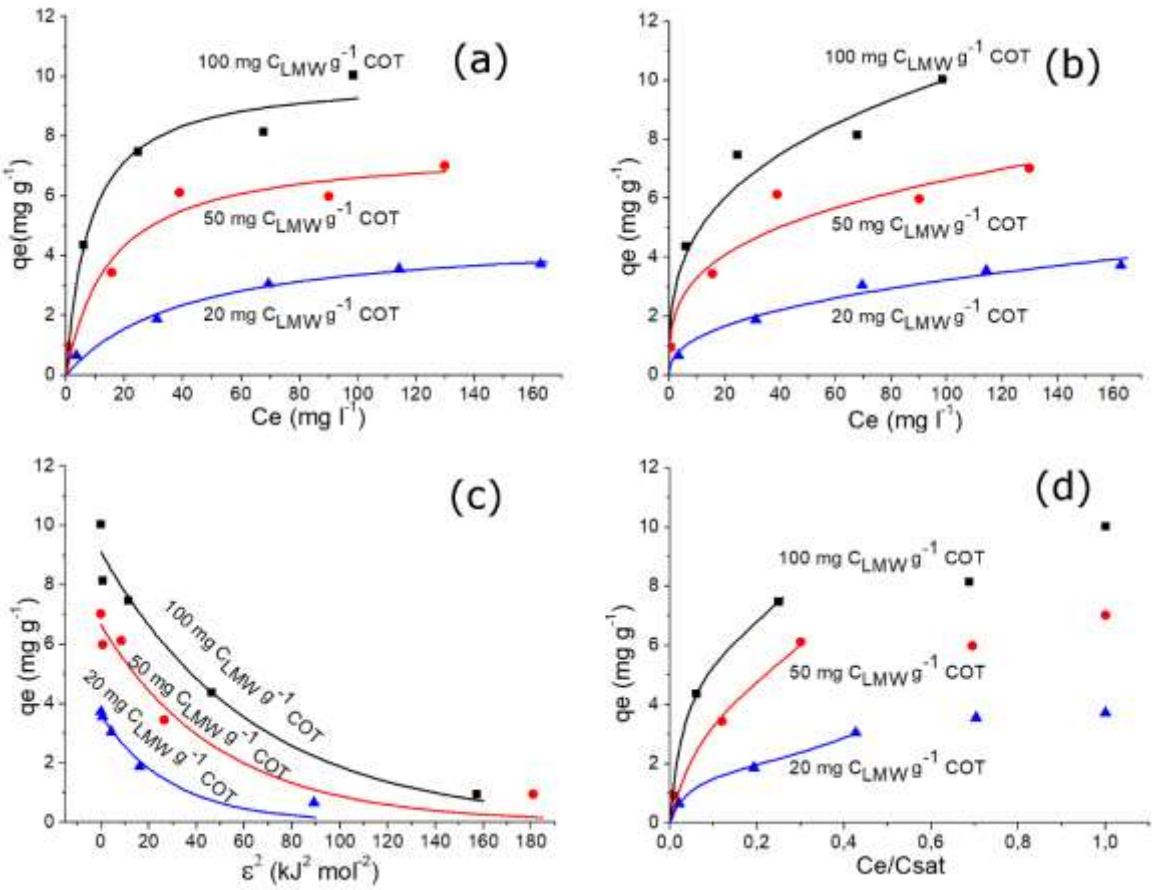

Figure 6. Nonlinear regressions of isotherm models: (a) Langmuir - Equation 4.2, (b) Freundlich - Equation 5.2, (c) D-R - Equation 6.2 and (d) BET - Equation 7.2. The main parameters of each nonlinear model and the values of RSS and *AIC* are reported in Table 3.

From these results, it is possible to say that the Langmuir model showed small differences in the parameter values when the linear and nonlinear regressions were employed. Therefore, the loss of information caused by linearization is not significant in this case and consequently both regressions can be used. On the other side, the loss of information caused by linearization in Freundlich and D-R was more significant than in Langmuir model and that aspect produced differences in the estimation of parameters. However, this loss of information can be reduced when the add-on of chitosan decreases, which leads to similar results for parameters as K_f, n and q_m in linear and nonlinear equations.

On the other hand, D-R model is applied to express the adsorption mechanism with Gaussian energy distribution onto a surface. This approach is usually applied to distinguish a physical adsorption from a chemical adsorption with the value of the most probable energy of adsorption

(E) or mean free energy. Nevertheless, this equation was initially used for adsorption from the gas phase [38]. The typical value of ion exchange is between 8 and 16 kJ mol^{-1} [52], hydrogen bonds have energy of 4 – 13 kJ mol^{-1}, and Van der Waals interactions have typical energy from 2 to 4 kJ mol^{-1} [53]. From this point of view, the value of E calculated for the adsorption corresponded mainly to a physisorption process with hydrogen bonds interactions in all investigated cases.

BET isotherm model was carried out considering only $C_e/C_{sat} < 0.45$; as a result, an accurate adsorption isotherm was obtained. Similar value of adsorption capacity (q_m) from this model was obtained in both linear and nonlinear regression. Successively, the values of q_m from linear regression were used to determination of the specific surface area of Cr (VI) ions on adsorbent as reported in literature [41, 42].

Table 4. Adsorption capacity (mg Cr (VI) g^{-1} C_{LMW}), cross-sectional area and specific surface area

		σ_1 (m^2 $molecule^{-1}$)	σ_2 (m^2 $molecule^{-1}$)	σ_3 (m^2 $molecule^{-1}$)
		2.12×10^{-19}	2.05×10^{-19}	2.83×10^{-19}
mg C_{LMW} g^{-1} COT	$q_{m,BET}$ (mg Cr (VI) g^{-1} C_{LMW})	$A_{s,1}$ (m^2 g^{-1} C_{LMW})	$A_{s,2}$ (m^2 g^{-1} C_{LMW})	$A_{s,3}$ (m^2 g^{-1} C_{LMW})
20	93.7	101.3	98.1	136.4
50	93.4	100.9	97.7	135.9
100	67.8	73.3	71.0	98.7

Table 4 reports the estimated values of cross sectional area (for one molecule of $HCrO_4^-$ in three different ways), q_m in terms of the mass of chitosan (mg Cr (VI) g^{-1} C_{LMW} instead of mg Cr (VI) g^{-1} COT-C_{LMW}) and the specific surfaces areas used for the adsorption of Cr (VI) ions. As this table shows, when adsorption capacity is calculated taking the mass of chitosan only into account, the resulting value increases considerably. These values were much higher in comparison with pure chitosan under the similar conditions: low molecular weight (7.9 mg Cr (VI) g^{-1} C_{LMW}) [52] and high molecular weight (24 mg Cr (VI) g^{-1} C_{HMW}) [54]. The experiment demonstrated the efficiency of grafted chitosan on the surface of cotton gauze. In addition, the specific surface area calculated by using different cross-sectional area showed similar results. Nevertheless, when the Van der Waals radius was considered, the area value was overestimated in comparison with the other two methods.

The values of specific surface area were also expressed per mass of cotton and divided per the specific surface area reported in literature for pure cotton fibres, 34 m^2 g^{-1} COT, ($A_{T,COT}$) [55–57]. It

was done in order to approach the percentage of the area occupied by the adsorption of Cr (VI) in relation to an initial area; the results are reported in Table 5.

Table 5. Percentage of area occupied by Cr (VI) ions

mg C_{LMW} g^{-1} COT	$As_{1,COT}/A_{T,COT}$ (% m^2/m^2)	$As_{2,COT}/A_{T,COT}$ (% m^2/m^2)	$As_{3,COT}/A_{T,COT}$ (% m^2/m^2)
20	6.0	5.8	8.8
50	14.8	14.4	20.0
100	21.6	20.9	29.0

As Table 5 shows, the percentage of the area occupied by active sites to adsorb chromium ions is approximatively between 6 and 24 % depending on the amount of chitosan: 7, 13 and 20 % for 20, 50 and 100 mg C_{LMW} g^{-1} COT, respectively. Consequently, in order to increase this percentage, the presence of higher number of amine groups on the surface or the ability of the other functional groups (-OH) to absorb Cr (VI) ions would be necessary. Otherwise, the percentage of occupied area would be close to the range mentioned above and the total area would not be employed.

CONCLUSIONS

A cotton gauze functionalized with chitosan was tested as an adsorbent for the removal of Cr (VI) ions from aqueous solutions in batch process. Results reported that grafted chitosan had higher adsorption capacity in comparison with the results for pure chitosan reported in literature. The results of kinetic adsorption show that an add-on of 100 mg C_{LMW} g^{-1} COT reaches a kinetic rate of pseudo-second order while an add-on of 20 and 50 mg C_{LMW} g^{-1} COT evidences a kinetic rate of pseudo-first order. Adsorption isotherm models Type II (IUPAC classification) with physisoprtion and monolayer formation were verified in all add-on cases (20, 50 and 100 mg C_{LMW} g^{-1} COT) by Langmuir model. From the value of the most probable energy of adsorption (D-R model) was deduced that physisorption process is carried out through hydrogen bonds interactions. Similar values for specific surface area were obtained considering three different cross-sectional areas and the results reported that the surface area employed to adsorb chromium ions is approximatively between 6 and 24% depending on the amount of chitosan.

Acknowledgements

This research did not receive any specific grant from funding agencies in the public, commercial, or not-for-profit sectors.

REFERENCES

[1] OSHA (Occupational Safety and Health Administration), "Hexavalent Chromium," *United States Department of Labor*, **2019**, accessed on 12 June 2019 https://www.osha.gov/SLTC/hexavalentchromium/index.html

[2] D.M. Hausladen, A.Alexander-Ozinskas, C. McClain, S. Fendorf, *Environ. Sci. Technol.* **2018**, *52*, 8242.

[3] A. Zhitkovich, *Chem. Res. Toxicol.* **2011**, *24*, 1617.

[4] IARC (International Agency for Research on Cancer), "Chromium (VI) compounds – 2.Cancer in humans," *IARC Monographs on the evaluation of carcinogenic risks to humans – Arsenic, Metals, Fibres, and Dusts*. Lyon **2012**, accessed on 07 October 2019, https://publications.iarc.fr/120

[5] M. Costa, *Crit. Rev. Toxicol.* **1997**, *27*, 431.

[6] P.B.Tchounwou, C.G. Yedjou, A.K. Patlolla, D.J. Sutton, *Mol. Clin. Environ. Toxicol.* **2012**, *101*, 133.

[7] WHO (World Health Organization), "Chromium. Section 12. Chemical fact sheets," *Guidelines for drinking-water quality: fourth edition incorporating the first addendum*, 4th edn. Geneva **2017**, accessed on 03 October 2019, https://www.who.int/water_sanitation_health/publications/drinking-water-quality-guidelines-4-including-1st-addendum/en/

[8] D.I. Koilakos, *Water* **2017**, *9*, 611.

[9] B.A. Shah, A.V. Shah, R.R. Singh, *Int. J. Environ. Sci. Techol.* **2009**, *6*, 77.

[10] A.A. Siti Nur, S.I. Mohd Halim, M.D. Lias Kamal, I. Shamsul, *World Appl. Sci. J.* **2013**, *28*, 1518.

[11] M.N.V. Ravi Kumar, *React. Funct. Polym.* **2000**, *46*, 1-27.

[12] M.W. Wan, C.C. Kan, B.D. Rogel, M.L.P. Dalida, *Carbohydr. Polym.* **2010**, *80*, 891.

[13] R. Bassi, S.O. Prasher, B.K. Simpson, *Sep. Sci. Technol.* **2000**, *35*, 547.

[14] M. Vandenbossche, M. Jimenez, M. Casetta, S. Bellayer, A. Beaurain, S. Bourbigot, M. Traisnel, *React. Funct. Polym.* **2013**, *73*, 53.

[15] F. Ferrero, M. Periolatto, *J. Nanosci. Nanotechnol.* **2011**, *11*, 8663.

[16] A.L. Andrady, A. Torikay, T. Kobatake, *J. Appl. Polym. Sci.* **1996**, *62*, 1465.

[17] F. Ferrero, M. Periolatto, C. Vineis, A. Varesano, *Carbohydr. Polym.* **2014**, *110*, 207.

[18] M.R. Kasaai, J. Arul, G. Charlet, *J. Polym. Sci. Part B: Polym. Phys.* **2000**, *38*, 2591.

[19] F. Ferrero, C. Tonetti, M. Periolatto, *Carbohydr. Polym.* **2014**, *110*, 367.

[20] F.T. Giachet, M. Periolatto, D.O. Sanchez Ramirez, R.A. Carletto, A. Varesano, C. Vineis, R. Bongiovanni, *J. Ind. Text.* **2019**, *48*, 1384.

[21] R.L. Tseng, F.C. Wu, R.S. Juang, *J. Taiwan Inst. Chem. Eng.* **2010**, *41*, 661.

[22] Y.S. Ho, *Scientometrics* **2004**, *59*, 171.

[23] S. Lagergren, *Kungliga Svenska Vetenskapsakademiens* **1898**, *24*, 1.

[24] W. Plazinski, J. Dziuba, W. Rudzinski, *Adsorption* **2013**, *19*, 1055.

[25] Y.S. Ho, *J. Hazard. Mater.* **2006**, *136*, 681.

[26] Y.S. Ho, G. McKay, *Process. Biochem.* **1999**, *34*, 451.

[27] I. Langmuir, *J. Am. Chem. Soc.* **1918**, *40*, 1361.

[28] H. Freundlich, *Z. Phys. Chem.* **1906**, *57*, 385.

[29] H. Freundlich, *Kapillarchemie. Academishe Bibliotek, Leipzing*. **1909**

[30] M.M. Dubinin, L.V. Radushkevich, *Proc. Acad. Sci. USSR Phys. Chem. Sect.* **1947**, *55*, 331.

[31] N.D. Hutson, R.T. Yang, *Adsorption* **1997**, *3*,189.

[32] G.F. Cerofolini, *J. Low Temp. Phys.* **1972**, *6*, 473.

[33] K.Yang, W. Wu, Q. Jing, L. Zhu, *Environ. Sci. Technol.* **2008**, *42*, 7931.

[34] M.M. Dubinin, *Chem. Rev.* **1960**, *60*, 235.

[35] M.M. Dubinin, *Carbon* **1985**, *23*, 373.

[36] E. Fernandez, D. Hugi-Cleary, M.V. Lopez-Ramon, F. Stoeckli, *Langmuir* **2003**, *19*, 9719.

[37] B. Pan, H. Zhang, *Environ. Sci. Technol.* **2014**, *48*, 6772.

[38] J.P. Hobson, *J. Phys. Chem.* **1969**, *73*, 2720.

[39] S. Brunauer, P.H. Emmett, E. Teller, *J. Am. Chem. Soc.* **1938**, *60*,309.

[40] J.G. Choi, D.D. Do, H.D. Do, *Ind. Eng. Chem. Res.* **2001**, *40*, 4005.

[41] M. Thommes, K. Kaneko, A.V. Neimark, J.P. Oliver, F. Rodriguez-Reinoso, J. Rouquerol, K.S.W. Sing, *Pure Appl. Chem.* **2015**.

[42] H.K. Livingston, *J. Am. Chem. Soc.* **1944**, *66*, 569.

[43] M.K. Ismail, *Langmuir* **1992**, *8*, 360.

[44] P.H. Emmett, S. Brunauer, *J. Am. Chem. Soc.* **1937**, *59*, 1553.

[45] C.L. Yaws, "Table 1. Physical properties – inorganic compoundsm," *Yaws' Critical Property Data for Chemical Engineers and Chemist*, Knovel, **2012**, accessed on 12 June 2019, http://app.knovel.com/hotlink/toc/id:kpYCPDCECD/yaws-critical-property/yaws-critical-property

[46] J.H. Jensen, J.C. Kromann, *J. Chem. Educ.* **2013**, *90*, 1093.

[47] P. Pyykkö, M. Atsumi, *Chem.-Eur. J.* **2008**, *15*, 186.

[48] A. Bondi, *J. Phys. Chem.* **1964**, *68*, 441.

[49] R.K. Tandon, P.T. Crisp, J. Ellis, *Talanta* **1984**, *31*, 227.

[50] N.K. Hamadi, X. Dong Chen, M.M. Farid, M.G.Q. Lu, *Chem. Eng. J.* **2001**, *84*, 95.

[51] K.S.W. Sing, D.H. Everett, R.A.W. Haul, L. Moscou, R.A. Pierotti, J. Rousquérol, T. Siemieniewska, *Pure Appl. Chem.* **1985**, *57*, 603.

[52] Y.A. Aydin, N.D. Aksoy, *Chem. Eng. J.* **2009**, *151*, 188.

[53] J.M.Berg, J.L. Tymoczko, L. Stryer, "Chemical bonds in biochemistry. Section 1.3," *Biochemistry*, 5th edn. W.H. Freeman, New York **2002**, accessed on 12 June 2019, http://www.ncbi.nlm.nih.gov/books/NBK22567

[54] R. Schmuhl, H.M. Krieg, K. Keizer, *Water S.A.* **2001**, *27*, 1.

[55] C. Kaewprasit, *Text. Res. J.* **2004**, *74*, 730.

[56] L.I. Mikhalovska, V.M. Gun'ko, A.A. Rugal, O.I. Oranska, Y.I. Gornikov, C. Morvan, N. Follain, C. Domas, E.M., Pakhllov, S.V. Mikhalovsky, *RSC Adv.* **2012**, *2*, 2032.

[57] S.H. Zeronian, *AATCC Rev.* **2015**, *15*, 36.